Optics Letters

Optical trapping and micromanipulation with a photonic lantern-mode multiplexer

Amado M. Velázquez-Benítez,[1,*] K. Yanín Guerra-Santillán,[2] Raúl Caudillo-Viurquez,[2] J. Enrique Antonio-López,[3] Rodrigo Amezcua-Correa,[3] and Juan Hernández-Cordero[4]

[1]Centro de Ciencias Aplicadas y Desarrollo Tecnológico, UNAM, Cd. Universitaria, Mexico City 04510, Mexico
[2]Facultad de Ciencias, Universidad Nacional Autónoma de México, Mexico City 04510, Mexico
[3]CREOL, The College of Optics and Photonics, the University of Central Florida, Orlando, Florida 32816, USA
[4]Instituto de Investigaciones en Materiales, UNAM, Cd. Universitaria, Mexico City 04510, Mexico
*Corresponding author: amado.velazquez@ccadet.unam.mx

Received 13 December 2017; revised 1 February 2018; accepted 9 February 2018; posted 12 February 2018 (Doc. ID 315227); published 12 March 2018

We demonstrate a simple approach based on a photonic lantern spatial-mode multiplexer and a few-mode fiber for optical and manipulation of multiple microspheres. Selective generation of linearly polarized (LP) fiber modes provides light patterns useful for trapping one or multiple microparticles. Furthermore, rotation of the particles can be achieved by switching between degenerate LP modes, as well as through polarization rotation of the input light. Our results show that emerging fiber optic devices such as photonic lanterns can provide a versatile and compact means for developing optical fiber traps.

OCIS codes: (350.4855) Optical tweezers or optical manipulation; (060.2340) Fiber optics components; (060.1810) Buffers, couplers, routers, switches, and multiplexers; (030.4070) Modes.

https://doi.org/10.1364/OL.43.001303

Since the first demonstration of particle trapping by Ashkin, the use of light for object manipulation at the micro- and nanometric scale has attracted a lot of attention [1,2]. Transparent-dielectric particle trapping relies on momentum transfer from the photons to the particles, acting through scattering and gradient forces [1–3]. While the scattering force pushes the particles in the direction of propagation, the gradient force, arising from the gradient of the electric field, pushes the particles toward the direction of increasing intensity. Optical trapping is achieved upon balancing these forces, which can be achieved through beam shaping and control [4–7]. These approaches have further provided means for dynamic repositioning of the trapped particles using reconfigurable light patterns. Structured optical beams, such as Laguerre–Gauss and Hermit–Gauss modes, have been obtained using phase masks and bulk optical components [3,4]. Spatial light modulator (SLM) technology has also emerged as a suitable tool to generate complex and dynamic light patterns [5,6]. In spite of their functionality, these approaches usually result in bulky setups requiring careful alignment of multiple optical elements. In contrast, the use of optical fibers is a feasible approach to achieve optical trapping using simpler experimental arrangements [7]. Aside from single-mode fibers (SMFs), which can readily provide a single spot for particle trapping, tailored spatial light patterns for capturing multiple particles have been obtained using multimode fibers (MMFs) combined with a SLM [8]. Extended capabilities have also been explored with arrays of multiple fibers and multicore fibers [9,10]. Other approaches make use of few-mode fibers (FMFs) by modifying the excitation of the LP modes [11–13]. Nonetheless, these approaches can involve complicated fabrication methods, and the resulting devices do not provide a simple means to tailor the generated light patterns on-demand.

Recent research in astrophotonics and optical communications has turned to using space division multiplexing for addressing signals based on spatial modes [14–16]. Photonic lanterns (PLs) are now considered one of the most versatile mode multiplexers, capable of addressing a large number of LP fiber modes. These devices are either built by tapering a bundle of SMFs in order to create a MMF at the device output [Fig. 1(a)], or by inscribing multiple planar waveguides through direct laser writing [14–16]. Interestingly, mode selectivity can be tailored in PLs, making it possible to address individual LP modes at the multimode output through each of the SMFs' inputs [15,17,18]. This feature is useful for exciting specific modes in FMFs, which can support propagation of independent LP modes with reduced crosstalk, thus providing an attractive platform for spatial division multiplexed communication systems [15,19–21]. PLs mode multiplexers are also finding very interesting applications in diverse areas, including, among others, lasers and sensors [18,22–24]. In this work, we demonstrate the use of all-fiber photonic lanterns for the generation of structured light patterns for applications in optical trapping and manipulation of microparticles.

Figure 1(a) depicts an all-fiber photonic lantern with modal selectivity capable of exciting the LP_{01} and LP_{11} modes. The PL used for our experiments was fabricated following the methodology described elsewhere [14–16,18]. In this particular case,

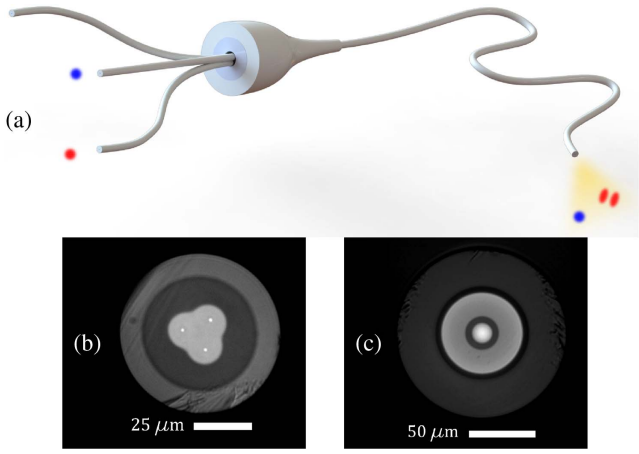

Fig. 1. (a) Illustration of the photonic lantern (PL) fusion spliced to a few-mode fiber (FMF). Cleaved end facets of (b) the PL and (c) the FMF used for the experiments.

we used fibers with two different core diameters (10 μm and 8.2 μm) in order to generate the desired mode selectivity [17,18]. The cleaved end at the taper waist of the PL resulted in a MMF with a numerical aperture (NA) of 0.15, an outer diameter of 65 μm, and a core diameter of 21 μm, as shown in Fig. 1(b). The MMF end of the photonic lantern was then spliced to two meters of a 2-LP FMF with a cladding diameter of 125 μm and core diameter of 15 μm, as is illustrated in Fig. 1(c).

While using the larger core input fiber yielded the LP_{01} mode, light launched at the other two input fibers produced two degenerate LP_{11} modes. The measured far-field intensity profiles at the output of the 2 m long FMF are presented in Fig. 2(a). These were obtained using a superluminescent diode ($\lambda = 1550$ nm) launched through each of the input SMFs. The camera images indicate low mode scrambling, yielding high-purity LP_{01} and LP_{11} modes. Analysis of the intensity distribution of the LP_{11} modes yields a contrast of 11 dB for the LP_{11} modes [Fig. 2(b)] and a Gaussian-like beam distribution. The mode effective areas for the LP_{01} and LP_{11} in this fiber

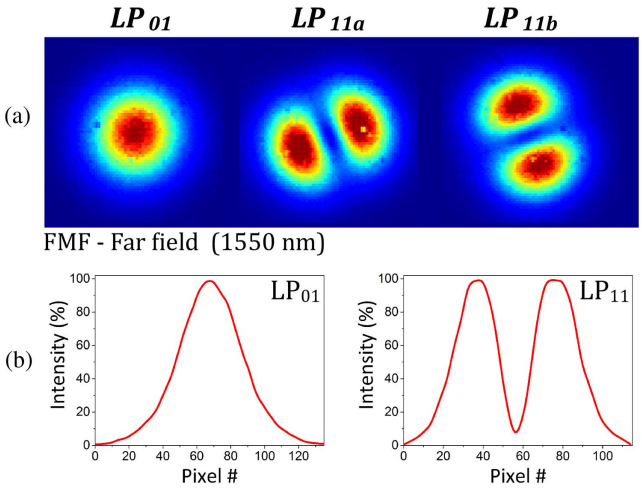

Fig. 2. (a) Far-field mode profiles at the output of the FMF and (b) the intensity distribution profiles of the generated modes.

have been measured to be approximately 155 μm^2 and 159 μm^2, respectively [19]. The insertion losses for the PL were around 0.2 dB for each of the input fibers. After splicing the PL to the FMF, the resulting losses were 0.3 dB for the LP_{01} mode and 1 dB for the LP_{11} modes, arising mostly from the core mismatch between the PL and the FMF. Similar devices have demonstrated lower losses by a correct core matching splice [25].

Optical trapping and manipulation of dielectric particles was performed using the setup shown in Fig. 3. A laser diode ($\lambda = 1550$ nm) was coupled to the inputs of the PL, while the output end of the FMF was mounted on a translation stage and inserted in a cuvette housing a solution of deionized water with dispersed microparticles. Two solutions were prepared using different microparticles: silica spheres with diameters of ≈8 μm, and polystyrene spheres with an average diameter of ≈4.8 μm. These sizes were chosen aiming at trapping two or more particles with the different beam profiles available. The modal pattern at the output end was varied using a fiber-optic polarization synthesizer (PSY-101, General Photonics) and an optical-fiber polarization beam-splitter (PBS) connected to the SMFs of the PL, as is illustrated in Fig. 3. With this arrangement, and owing to the modal selectivity of the PL, each of the two degenerate LP_{11} modes can be readily obtained simply by changing the polarization state in the synthesizer. For visualization, we used a charge-coupled device (CCD) camera (PL-B954U, Pixelink) and a 20× apochromatic long-working-distance microscope objective (0.42 NA). With this configuration, we obtained a side view of the FMF end face, and alternatively, we also gained access to a frontal view upon placing a tilted mirror at the bottom of the cuvette (not shown in the figure).

Optical trapping of the larger microparticles (8 μm) was first achieved using a fixed polarization state and launching the LD separately through all the different SMFs. As shown in Figs. 4(a) and 4(b), a single particle was readily captured when exciting the LP_{01} mode. In contrast, the generation of the LP_{11} mode allowed for trapping two particles simultaneously [see Figs. 4(c) and 4(d)], owing to the two intensity maxima inherent to this mode profile. Although the intensity between the maxima of the generated LP_{11} mode is not fully reduced to zero, the contrast is sufficient to produce simultaneous trapping of two particles. For both cases, the output power required for

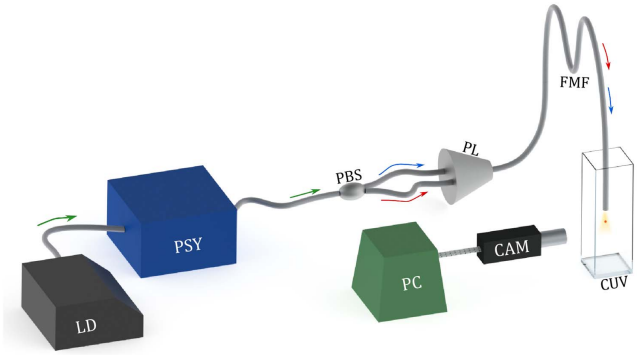

Fig. 3. Experimental setup for optical trapping and manipulation of microparticles. LD, laser diode; PSY, polarization synthesizer; PBS, optical-fiber polarization beam splitter; PL, photonic lantern; FMF, few-mode fiber; PC, computer; CAM, CCD camera; CUV, cuvette.

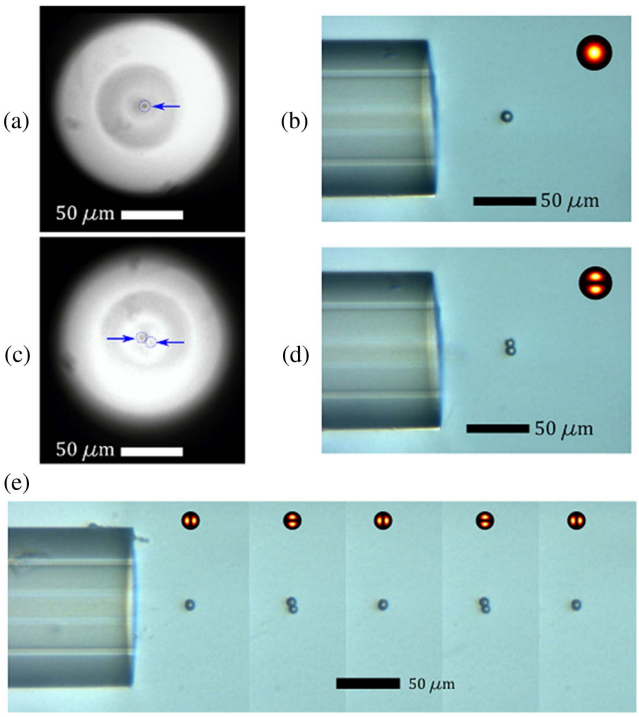

Fig. 4. Particle trapping with the LP_{01} [frontal view (a) and side view (b)] and LP_{11} modes [frontal view (c) and side view (d)] generated in the FMF output; blue arrows indicate the trapped particles. Sequence of images (e) showing that particles trapped with the LP_{11} mode can be rotated through polarization rotation (Visualization 1). The insets depict the mode profiles observed at the frontal plane and their orientation at the output of the FMF.

particle trapping was within 28–40 mW, as measured form the output of the FMF. Further noticeable effects in the particle solution included thermal convection currents toward the fiber end attributed to water absorption [26]. Nonetheless, particle trapping was sustained under these experimental conditions.

Manipulation of the trapped particles was explored by alternating between both of the two LP_{11} degenerate modes. Because the fibers producing the LP_{11} degenerate modes were connected to the PBS outputs, switching between these modes was readily performed with the polarization synthesizer. In particular, changes between two orthogonal linear polarization modes produced switching between the intensity patterns obtained with the LP_{11a} and LP_{11b} modes [see Fig. 2(a)]. Hence, once the particles were trapped, the synthesizer was set to produce polarization switching between orthogonal states, thus yielding microparticle displacement. Figure 4(e) includes a sequence of images acquired while switching between the degenerate LP_{11} modes, showing that the microparticles effectively rotate by 90° during this process. When switching back and forth between the LP_{11} modes, the microparticles alternated their location between orthogonal positions within the capture zone (see Visualization 1). The particles hence remained trapped within the vicinity of the maxima of the degenerate fiber modes, and their positions were modified simply through polarization switching.

The effects of the polarization of the input beam on microparticle manipulation were further explored upon removing the PBS from the experimental setup. With this modification, linearly polarized light was launched separately into both of the SMFs exciting the degenerate LP_{11} modes of the PL. In this case, the polarization synthesizer was programmed to provide a continuous rotation of the linearly polarized input signal. As a result, we were able to continuously rotate the intensity patterns, albeit retaining the characteristic spatial distribution of the LP_{11} modes. This is due to the circular symmetry of the PL-FMF arrangement, allowing for the modal patterns to remain with slight modifications due to mode mixing during polarization rotation [15,16,18,25]. Once two microparticles were trapped, they were readily rotated in a continuous fashion upon varying the orientation of the linearly polarized states. The sequence of images shown in Fig. 5 illustrates this effect; further evidence of particle rotation can also be seen in Visualization 2. This rotation effect was achieved using either the LP_{11a} or LP_{11b} modes of the PL. It is worthwhile to note that particle rotation occurs slightly out of the transversal plane (i.e., the plane perpendicular to the fiber axis). We attribute this to slight imperfections of the PL-FMF arrangement, which may produce changes in the relative intensities of the two maxima regions of the LP_{11} modes during rotation. In addition, the observed thermal convection may also play a role on this slight out-of-plane displacement of the particles.

We finally explored the optical trapping effects when using smaller particles (4.8 μm). Given the mode effective areas of the two maxima obtained from the LP_{11} modes, we expected to achieve the conditions for capturing several particles of smaller diameter, as observed using tapered fibers in microfluidic channels [26]. When using the LP_{01} mode, and FMF output powers as low as 6 mW, a single microparticle was initially trapped. After a few seconds, more particles were confined within the same area. Figure 6(a) illustrates multiple particle trapping in two separate regions with a small gap in between, as defined by the two lobes of the LP_{11} mode. Given the flow induced by thermal effects, optical and hydrodynamic forces seem to balance under this irradiation condition, and multiple microparticles can be trapped [26]. Owing to their larger mode effective area, the LP_{11} intensity pattern yielded more stable trapping conditions, with the microparticles resembling a closed-packed configuration toward the optical axis of the FMF. Figure 6(b) includes a sequence of images showing that up to six microparticles were captured and rotated with our experimental arrangement (see Visualization 3). As before, rotation of the microparticles was achieved through rotation of the linearly polarized beam launched into the input SMF.

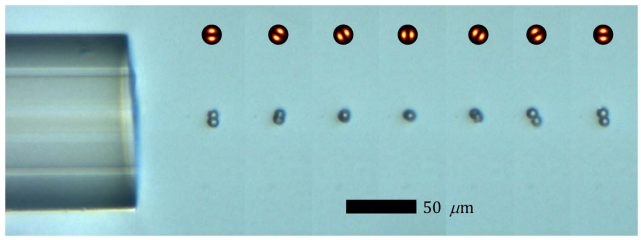

Fig. 5. Sequence of images showing the rotation of the 8 μm borosilicate microparticles by adjusting the polarization of the signal at one of the PL inputs corresponding to the LP_{11a} spatial mode (Visualization 2). The inset depicts the orientation of the mode profile at the output of the FMF.

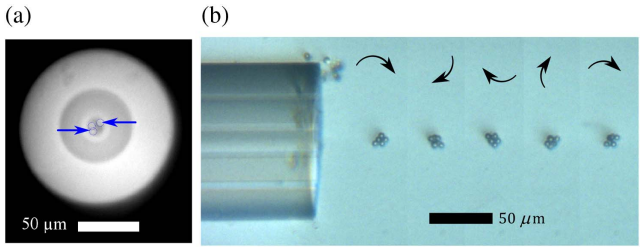

Fig. 6. Optical trapping of 4.8 μm polystyrene microparticles. (a) Front view of the fiber showing two trapping regions corresponding to the lobes of the LP_{11a} mode. (b) Rotation of the microparticles cluster by adjusting the polarization of the signal in one of the PL inputs corresponding to the LP_{11a} spatial mode (Visualization 3). The arrows indicate the particle rotation observed at the frontal plane.

It is clear from our results that all-fiber devices for spatial multiplexing provide a means to generate useful modal structures for particle trapping. The modal selectivity of the PL plays an important role in defining the zones for particle trapping. In particular, the generated LP_{11} mode prescribes two zones for particle trapping [see Fig. 6(a)]. A reduction in modal selectivity would lead to crosstalk, thereby modifying the generated light pattern and thus the trapping zone.

In conclusion, we have demonstrated the use of mode-selective PLs together with FMFs for trapping and rotation of microparticles. This emerging waveguide technology provides a straightforward manner for generating specific mode profiles useful for trapping several particles simultaneously. The correct selection of a specific LP mode grants a means for particle trapping with specific spatial distribution and orientation. Upon adjusting the polarization of the input beam, the modal intensity patterns obtained with these devices can be rotated, thus providing a simple means to change the position of the trapped particles. In particular, with our experimental setup we were able to trap and manipulate two particles by launching an LP_{11} mode. We further demonstrated the rotation of clusters of microparticles through rotation of a linearly polarized input beam. Advances in the fabrication of mode-selective PLs supporting a larger number of modes will undoubtedly offer further options for developing compact and versatile arrangements for microparticle manipulation.

Funding. DGAPA-UNAM (PAPIIT IT101215); National Science Foundation (NSF) (ECCS-1711230).

REFERENCES

1. A. Ashkin, J. M. Dziedzic, J. E. Bjorkholm, and S. Chu, Opt. Lett. **11**, 288 (1986).
2. M. Dienerowitz, M. Mazilu, and K. Dholakia, J. Nanophoton. **2**, 021875 (2008).
3. K. Dholakia, P. Reece, and M. Gu, Chem. Soc. Rev. **37**, 42 (2008).
4. P. A. Prentice, M. P. MacDonald, T. G. Frank, A. Cuschieri, G. C. Spalding, W. Sibbett, P. A. Campbell, and K. Dholakia, Opt. Express **12**, 593 (2004).
5. D. G. Grier, Nature **424**, 810 (2003).
6. M. Woerdemann, C. Alpmann, M. Esseling, and C. Denz, Laser Photon. Rev. **7**, 839 (2013).
7. A. Constable, J. Kim, J. Mervis, F. Zarinetchi, and M. Prentiss, Opt. Lett. **18**, 1867 (1993).
8. T. Čižmár and K. Dholakia, Opt. Express **19**, 18871 (2011).
9. A. L. Barron, A. K. Kar, T. J. Aspray, A. J. Waddie, M. R. Taghizadeh, and H. T. Bookey, Opt. Express **21**, 13199 (2013).
10. C. Liberale, G. Cojoc, F. Bragheri, P. Minzioni, G. Perozziello, R. La Rocca, L. Ferrara, V. Rajamanickam, E. Di Fabrizio, and I. Cristiani, Sci. Rep. **3**, 1258 (2013).
11. G. Volpe and D. Petrov, Opt. Commun. **237**, 89 (2004).
12. R. S. R. Ribeiro, R. Queirós, O. Soppera, A. Guerreiro, and P. A. Jorge, Photonics **2**, 634 (2015).
13. Y. Zhang, L. Zhao, Y. Chen, Z. Liu, Y. Zhang, E. Zhao, J. Yang, and L. Yuan, Opt. Commun. **365**, 103 (2016).
14. S. G. Leon-Saval, A. Argyros, and J. Bland-Hawthorn, Opt. Express **18**, 8430 (2010).
15. S. G. Leon-Saval, N. K. Fontaine, and R. Amezcua-Correa, Opt. Fiber Technol. **35**, 46 (2017).
16. T. A. Birks, I. Gris-Sánchez, S. Yerolatsitis, S. G. Leon-Saval, and R. R. Thomson, Adv. Opt. Photon. **7**, 107 (2015).
17. S. G. Leon-Saval, N. K. Fontaine, J. R. Salazar-Gil, B. Ercan, R. Ryf, and J. Bland-Hawthorn, Opt. Express **22**, 1036 (2014).
18. A. M. Velazquez-Benitez, J. C. Alvarado, G. Lopez-Galmiche, J. E. Antonio-Lopez, J. Hernández-Cordero, J. Sanchez-Mondragon, P. Sillard, C. M. Okonkwo, and R. Amezcua-Correa, Opt. Lett. **40**, 1663 (2015).
19. R. Ryf, S. Randel, A. H. Gnauck, C. Bolle, A. Sierra, S. Mumtaz, M. Esmaeelpour, E. C. Burrows, R. Essiambre, P. J. Winzer, D. W. Peckham, A. H. McCurdy, and R. Lingle, J. Lightwave Technol. **30**, 521 (2012).
20. P. Sillard, J. Lightwave Technol. **33**, 1092 (2015).
21. J. van Weerdenburg, A. Velázquez-Benitez, R. van Uden, P. Sillard, D. Molin, A. Amezcua-Correa, E. Antonio-Lopez, M. Kuschnerov, F. Huijskens, H. de Waardt, T. Koonen, R. Amezcua-Correa, and C. Okonkwo, Opt. Express **23**, 24759 (2015).
22. J. Montoya, C. Hwang, D. Martz, C. Aleshire, T. Y. Fan, and D. J. Ripin, Opt. Express **25**, 27543 (2017).
23. S. Wittek, R. Bustos Ramirez, J. Alvarado Zacarias, Z. Sanjabi Eznaveh, J. Bradford, G. Lopez Galmiche, D. Wang, W. Zhu, J. Antonio-Lopez, L. Shah, and R. Amezcua-Correa, Opt. Lett. **41**, 2157 (2016).
24. A. Van Newkirk, J. E. Antonio-Lopez, A. Velazquez-Benitez, J. Albert, R. Amezcua-Correa, and A. Schülzgen, Opt. Lett. **40**, 5188 (2015).
25. A. M. Velázquez-Benítez, J. E. Antonio-López, J. C. Alvarado-Zacarías, G. Lopez-Galmiche, P. Sillard, D. Van Ras, C. Okonkwo, H. Chen, R. Ryf, N. K. Fontaine, and R. Amezcua-Correa, "Scaling the fabrication of higher order photonic lanterns using microstructured preforms," in *European Conference on Optical Communication (ECOC)*, Valencia, Spain (2015), pp. 1–3.
26. J. T. Blakely, R. Gordon, and D. Sinton, Lab Chip **8**, 1350 (2008).